



AMORPHOUS Pd–P, Au–P AND Co–P ALLOYS AS CATHODE MATERIALS IN ALKALINE SOLUTION FOR OXYGEN REDUCTION

J. J. PODESTÁ and R. C. V. PIATTI

Instituto de Investigaciones Físicoquímicas Teóricas y Aplicadas (INIFTA), Facultad de Ciencias Exactas, Universidad Nacional de La Plata, Sucursal 4, Casilla de Correo 16, 1900 La Plata, Argentina

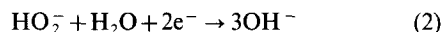
Abstract—The electrochemical behaviour of amorphous metal alloys (Pd_{96.4}P_{3.6}, Au_{94.0}P_{6.0} and Co_{94.6}P_{5.4} at.g%), prepared by electroless deposition technique, has been studied to test their suitability as low cost electrocatalysts for oxygen reduction (OR) in 1 M KOH aqueous solution at temperatures ranging from 30 to 70°C with different oxygen partial pressures. A rotating disc electrode (200–4000 rpm) was employed to obtain the current–potential quasi-steady state polarization curves and cyclic voltammograms due to the mixed activation–diffusion control. The reaction order with respect to oxygen was unity and the apparent number of electrons exchanged were four and two for OR on Pd_{96.4}P_{3.6} and Au_{94.0}P_{6.0} electrodes, respectively. A limiting kinetic current independent of the rotation rate was found on the Co_{94.6}P_{5.4} electrode, with an apparent activation energy of approximately 43 ± 5 kJ mol^{−1}. © 1997 International Association for Hydrogen Energy

NOMENCLATURE

M	Molar mass (g mol ^{−1})
η	Overvoltage (V)
F	Faraday constant (A s mol ^{−1})
j_{lim}	Limiting current density (A cm ^{−2})
j	Current density (mA cm ^{−2})
B	$0.62 n F c D^{2/3} \nu^{-1/6}$
c	Bulk concentration of dissolved oxygen (mol cm ^{−3})
D	Molecular diffusion coefficient of oxygen (cm ² s ^{−1})
ν	Kinematic viscosity (cm ² s ^{−1})
ω	Angular velocity (s ^{−1})
n	Number of transferred electrons per molecule of oxygen
m	Reaction order with respect to dissolved oxygen molecule
v	Sweep rate (V s ^{−1})
T	Absolute temperature (K)
E	Electrode potential (V)

but also of different branches of applied electrochemistry (energy conversion devices, fuel cells, possible use in the chlor–alkali industry, corrosion of metals and alloys and electrochemical sensors [1]). Excellent review papers concerning oxygen reduction (OR) on various kinds of electrode materials and proposed mechanisms have been published since the pioneering work of Damjanovic *et al.* [2–4].

As a first generalization, the OR process can be represented by the consecutive steps:



Reaction (1) is normally fast in the presence of a good electron transfer catalyst, whereas the subsequent reduction (2) is slow, requiring a good peroxide decomposition catalyst. The OR is an electrocatalytic surface process that is controlled to a large degree by adsorption and desorption. When oxygen molecules are present on the electrode surface in an undissociated form, the bond between oxygen and electrode surface is very weak. After the dissociation of the oxygen molecules into atoms, the strength of the bond between atomic oxygen and the cathode surface gradually increases. The dissociation of the molecule into atoms and their adsorption makes it possible for the OR process to occur directly in water (without an intermediate formation by hydrogen peroxide). The complete four electron process involves

1. INTRODUCTION

Intense worldwide interest in the investigation of oxygen ionization with different cathode materials in alkaline electrolytes is due to the importance of this process for the development not only of electrochemical kinetics,

two pathways and only one detectable intermediate species, the perhydroxide ion. These two processes may also occur simultaneously and their relative contributions to the total process vary with the electrode surface state and its potential. In practice, the measurement of OR rates in concentrated alkaline electrolytes is complicated by the low solubility of O_2 and subsequent smaller OR currents.

Among the different kinds of cathode materials, amorphous metallic alloys (AMA) possess very high catalytic or electrocatalytic activity which is superior to their crystalline counterparts in terms of their electrocatalysis [5–14]. The main objective of this study is to develop three binary amorphous alloys, Pd–P; Au–P and Co–P, prepared by the electrodeless deposition technique [15]. It is known that these metallic deposits, occurring as thin coatings on different substrates, reveal an amorphous structure as derived from XRD analysis. The selection of Pd, Au and Co as base metals of the binary alloys, as cathodes in oxygen electroreduction in alkaline solutions, results from the innumerable studies referring to the different mechanisms of the reaction and the catalytic behaviour reported in the literature [16]. The behaviour of the OR reaction on the three AMA electrodes is accounted for in this study via the electrochemical experimental results of steady polarization curves and cyclic voltammetry employing a rotating disc electrode due to the mixed activation–diffusion control.

2. EXPERIMENTAL DETAILS

2.1. Preparation of electrodes

Electroless metal alloy layers were prepared on SAE 1020 mild steel (C, 0.20; Si, 0.02; Mn, 0.58; S, 0.03; P, 0.03 balance Fe wt%) previously coated with the binary AMA; $Ni_{87.5}P_{12.5}$ at g% to improve adhesion [13]. The three AMA electrodeless deposits were obtained from the following aqueous solution composition and coating conditions:

AMA I ($Pd_{96.4}P_{3.6}$); 0.01 M $PdCl_2$ + 0.05 M HCl + 2.35 M NH_4OH + 0.50 M NH_4Cl + 0.10 M NaH_2PO_2 (pH 10.0), immersion time 2 h, thickness 5 μm , 55°C [15].

AMA II ($Au_{94.0}P_{6.0}$); 0.007 M $KAu(CN)_2$ + 1.40 M NH_4Cl + 0.14 M Na-citrate + 0.10 M NaH_2PO_2 (pH 7.0–7.5), immersion time 2 h, thickness 6 μm , 90°C [15].

AMA III ($Co_{94.6}P_{5.4}$); 0.10 M $CoSO_4 \cdot 6H_2O$ + 0.20 M NaH_2PO_2 + 0.20 M Na-citrate + 0.50 M H_3BO_3 (pH 8.0), immersion time 1 h, thickness 8 μm , 85°C [15].

The AMA deposits were employed as obtained having been first washed with distilled water, then with ethanol and finally rinsed with triply distilled water, dried at room temperature and stored in a dessicator. The chemical composition of the three coatings was determined by wet analysis on standard activated Al_2O_3 chips placed in the same conditions and simultaneously in the three electroless baths. The AMA I, II and III coatings on Al_2O_3 substrates were dissolved independently in 6 M HCl and 7 M HNO_3 to transform P to H_3PO_4 . Phosphorus content on each sample was determined as $(NH_4)_3P(Mo_3O_{10})_4$ with $(NH_4)_2MoO_4$ reagent. Pd and Au components of

AMA I and AMA II were gravimetrically determined as free metals by precipitation with H_2SO_3 as reducing agent from the acid treatment. Co in AMA III as analysed by atomic absorption spectroscopy.

2.2. Electrochemical characterization

Electrochemical experiments were carried out in a double walled pyrex glass cell with a separate compartment for the reference electrode, Hg/HgO/1 M KOH, connected with the main compartment via a Luggin–Haber capillary. Its tip was placed at about 0.3 cm below the middle of the rotating disc electrode (RDE). The potential of the reference electrode at different temperatures referred to as the SHE is 0.121 V at 30°C, 0.123 V at 50°C and 0.127 V at 70°C. Each working electrode (AMA I, II and III) consisted of SAE 1020 mild steel cylinders axially embedded in a cylindrical PTFE holder to obtain a metal disc of 1 cm^2 , to be coated with the AMA and used either still or under rotation. All current density values are given with respect to geometric surface area.

The RDE was tested by the reduction of a $K_3Fe(CN)_6/K_4Fe(CN)_6$ couple in an alkaline medium. It has been shown that the RDE behaves in accordance with the theoretical Levich equation [17]. A platinum wire of about 10 cm^2 geometric area inside a glass tube was used as the counter electrode, separated from the electrolyte by a porous fritted glass diaphragm. Electrochemical tests consisting of a quasi-steady state potentiostatic linear potential sweep technique with a scanning rate of 2×10^{-3} V s^{-1} for current–potential curves and cyclic voltammetry (CV) at potential sweep rates (v) ranging from 5×10^{-2} to 0.5 V s^{-1} covering different potential ranges at various rotation frequencies (200–4000 rpm), were used. As electrolyte, a 1 M KOH aqueous solution was made up using analytic reagent grade KOH pellets (0.2% carbonate) and triply distilled water under 0.20, 0.50, 0.75 and 1.0 atm of high purity oxygen (99.96%), or oxygen–nitrogen mixtures at 30, 50 and 70°C. No attempt was made to remove the carbonate initially present in the KOH.

3. RESULTS AND DISCUSSION

3.1. Polarization measurements with the RDE

3.1.1. Polarization curves for OR. Typical quasi-steady state cathodic polarization curves were obtained under potentiostatic conditions by linear potential sweep rate of 2×10^{-3} V s^{-1} at constant temperature with different rotation frequencies and oxygen partial pressures. These curves were recorded in the cathodic direction from the open circuit value to low potentials.

Figures 1–3 show the relationships between the overpotential η (V) and the logarithm of the current density j ($mA\ cm^{-2}$) in 1 M KOH at 30°C after saturating the electrolyte for 30 min with O_2 at 1.0 atm pressure, at rotation rates ranging from 200 to 4000 rpm for AMA I, II and III, respectively. The curves obtained are similar in shape, showing the appearance of a limiting current

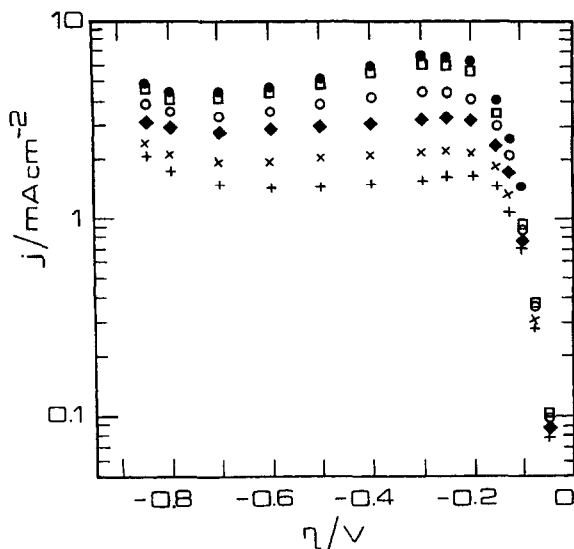


Fig. 1. Quasi-steady state polarization curves for OR on $\text{Pd}_{96.4}\text{P}_{3.6}$ in 1 M KOH solution at a scan rate $2 \times 10^{-3} \text{ V s}^{-1}$. Specified rotation rates: +, 200; x, 400; ◆, 800; ○, 1500; □, 3000 and ●, 4000 rpm, 30°C , O_2 1 atm.

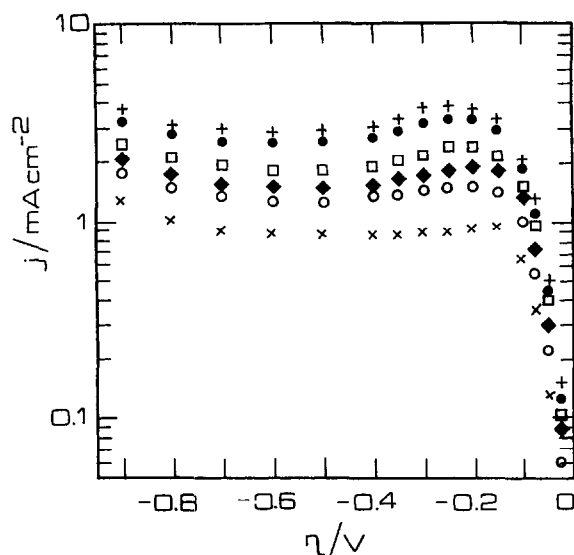


Fig. 2. Quasi-steady state polarization curves for OR on $\text{Au}_{94.0}\text{P}_{6.0}$ in 1 M KOH solution at a scan rate $2 \times 10^{-3} \text{ V s}^{-1}$. Specified rotation rates: x, 200; ○, 400; ◆, 800; □, 1500; ●, 3000 and +, 4000 rpm, 30°C , O_2 1 atm.

plateau dependent on the rotation rate with the exception of the AMA III electrode which shows a unique limiting current density value which is a function of the oxygen partial pressures but independent of the rotation rate. For the AMA I and AMA II cathodes, the well defined curves and the dependence of the reduction current on rotation rate indicate that the OR process is under mixed activation-diffusion control at all rotation rates exam-

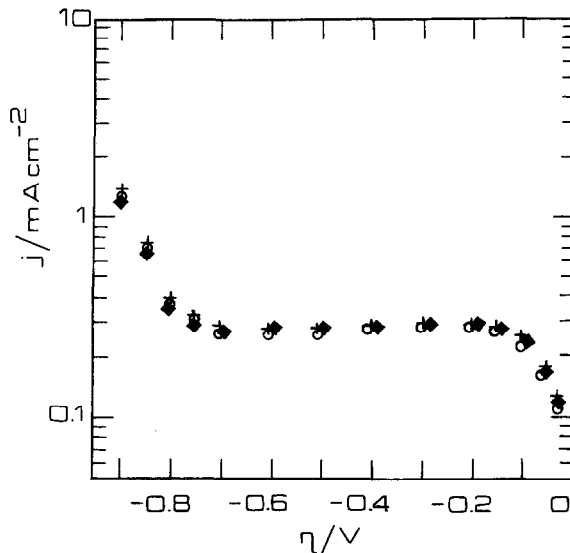


Fig. 3. Quasi-steady state polarization curves for OR on $\text{Co}_{94.6}\text{P}_{5.4}$ in 1 M KOH solution at a scan rate $2 \times 10^{-3} \text{ V s}^{-1}$. Specific rotation rates: ◆, 400; ○, 800 and +, 1500 rpm, 30°C , O_2 1 atm.

ined. According to these characteristics, analysis of the results obtained has been made.

3.1.2. Limiting current density. AMA I ($\text{Pd}_{96.4}\text{P}_{3.6}$) and AMA II ($\text{Au}_{94.0}\text{P}_{6.0}$) as cathodes for the OR process present limiting current densities dependent on the rotation rate suggesting their comparison with those calculated on the basis of Levich equation:

$$j_{\text{lim}} = 0.62 n F c D^{2/3} \nu^{-1/6} \omega^{1/2} \quad (3)$$

where n is the number of transferred electrons per oxygen molecule, F the Faraday constant, c the bulk concentration of dissolved oxygen, D the molecular diffusion coefficient of oxygen, ν the kinematic viscosity and ω , the angular velocity [18–20].

The following set of values were obtained for 1 M KOH solution at 30°C :

c , $0.80 \times 10^{-6} \text{ mol cm}^{-3}$ (1 atm), $0.61 \times 10^{-6} \text{ mol cm}^{-3}$ (0.75 atm), $0.47 \times 10^{-6} \text{ mol cm}^{-3}$ (0.50 atm) and $0.19 \times 10^{-6} \text{ mol cm}^{-3}$ (0.2 atm).

D , $1.57 \times 10^{-5} \text{ cm}^2 \text{ s}^{-1}$ and ν , 1.071×10^{-2} stokes gives different slopes of j_{lim} (A cm^{-2}) against $\omega^{1/2}$ ($\text{s}^{-1/2}$) for $n = 4$. These are presented in Fig. 4 for the AMA I ($\text{Pd}_{96.4}\text{P}_{3.6}$) electrode.

This good agreement between the experimental and calculated values indicates the direct four electron reduction where reoxidation and chemical decomposition of peroxy ions is absent. The behaviour of an AMA II ($\text{Au}_{94.0}\text{P}_{6.0}$) coated cathode is similar to that found for AMA I, but with different slope values with a value of $n = 2$ involving a couple of two electron-transfer-steps to water with hydrogen peroxide as the intermediate. As mentioned above, the independence of the limiting current with rotation rate at a constant oxygen partial pres-

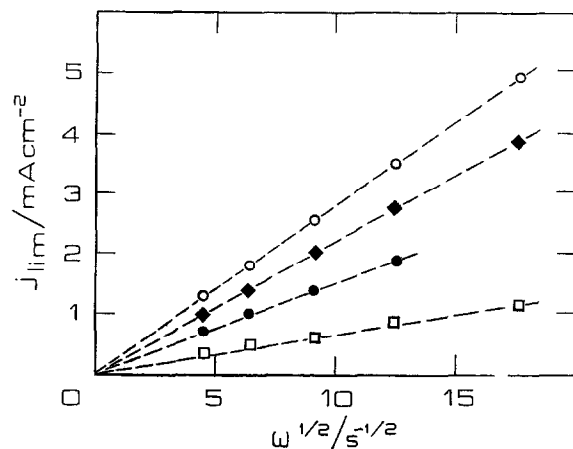


Fig. 4. Dependence of limiting current density of oxygen reduction on angular velocity on $Pd_{96.4}P_{3.6}$ in 1 M KOH solution at a scan rate $5 \times 10^{-3} V s^{-1}$ at specified oxygen partial pressures: \square , 0.2 atm; \bullet , 0.5 atm; \blacklozenge , 0.75 atm and \circ , 1 atm $30^\circ C$.

sure presented by the AMA III ($Co_{94.6}P_{5.4}$) makes it impossible to analyse applying Levich equation

3.1.3. *The reaction order with respect to O_2 .* The O_2 reduction current density (j) may be written as follows for a specified overpotential:

$$j = kc^m [j_{lim} - j/j_{lim}]^m \quad (4)$$

where k is the rate constant and m the reaction order. A plot of $\log j$ vs $\log(1 - j/j_{lim})$ should yield a straight line with a slope of m . Plots of this type are shown in Fig. 5 for the system AMA II ($Au_{94.0}P_{6.0}$) in 1 M KOH, oxygen partial pressure: 0.2 atm at $30^\circ C$. The values of j at all rotation rates were chosen at low overpotential values from the corresponding polarization cathodic curve. The slopes of these straight plots were mostly between 0.98 and 1.02, suggesting a first order reaction for OR. Similar

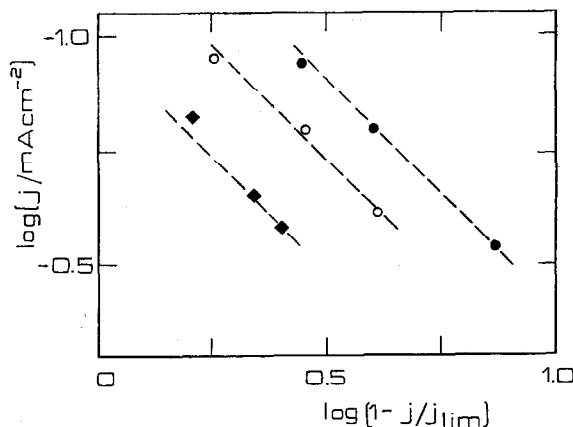


Fig. 5. Dependence $\log(j, mA cm^{-2})$ against $\log(1 - j/j_{lim})$, for oxygen reduction on $Au_{94.0}P_{6.0}$ in 1 M KOH solution, 0.2 atm oxygen partial pressure, $30^\circ C$. Values of j result from overpotential values: \blacklozenge , $-0.05 V$; \circ , $-0.075 V$ and \bullet , $-0.100 V$ at different rotation rates.

values were obtained with AMA I ($Pd_{96.4}P_{3.6}$) cathodes in 1 M KOH with the different oxygen partial pressures mentioned above.

Koutecky-Levich plots of $1/j$ vs $\omega^{-1/2}$ are shown in Fig. 6 for the same system as Fig. 5; reasonably parallel straight lines are obtained. The inverse of the slope of these lines yields a value for the Levich constant $B = 0.62 n F c D^{2/3} \nu^{-1/6}$ equal to $3.3 \times 10^{-5} A cm^{-2} s^{1/2}$ in good agreement with the calculated value according to equation (3) with a value of $3.1 \times 10^{-5} A cm^{-2} s^{1/2}$ under the assumption of $n = 2$.

3.2. Cyclic voltammetry

The CV experiments were performed by scanning the potential between -1.10 and $+0.70 V$ vs Hg/HgO/1 M KOH, with different sweep rates ν , ($5 \times 10^{-3} V s^{-1} \leq \nu \leq 0.50 V s^{-1}$) for the three AMAs. The voltammograms run with AMA I can be comparable to those already reported for polycrystalline palladium electrodes in base [21, 22].

For AMA II the voltammograms are comparable to those reported for a polycrystalline gold electrode in an alkaline medium [23]. The voltammograms with AMA III ($Co_{94.6}P_{5.4}$) electrodes are quite similar to the different amorphous cobalt-based alloys, exhibiting the same multiplicity of peaks [12, 13, 24, 25]. It is worth mentioning that poorly defined limiting currents were found for the AMA cathodes in the experimental conditions described above even at the lowest ν value. The evidence that the local process of oxygen ionization slows down as the amount of the phase oxides on the surface is increased is demonstrated when the voltammograms were performed by scanning the potential from the rest potential of each alloy in the cathodic direction. Figure 7 shows the CV of an amorphous $Pd_{96.4}P_{3.6}$ alloy in 1 M KOH at 0.5 atm oxygen pressure, $30^\circ C$ and with a rotation rate of 200 rpm at sweep rates ν marked on the curves. Two limiting current plateaus for the two- and four-electron (sequential) reduction are very well-defined for this system, but

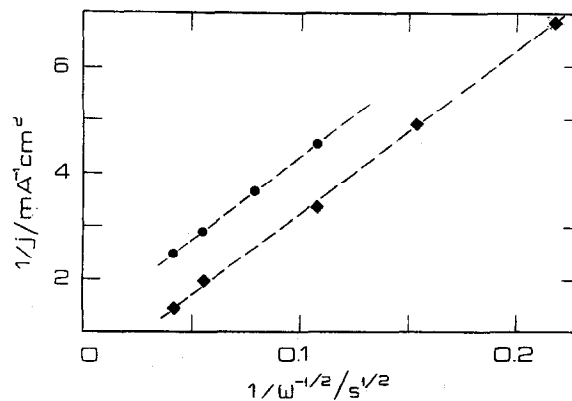


Fig. 6. Dependence $1/j$ against $\omega^{-1/2}$ for oxygen reduction on $Au_{94.0}P_{6.0}$ in 1 M KOH solution, 0.2 atm oxygen partial pressure, $30^\circ C$. Values of j result from overpotential values: \bullet , $-0.05 V$ and \blacklozenge , $-0.075 V$ at different rotation rates.

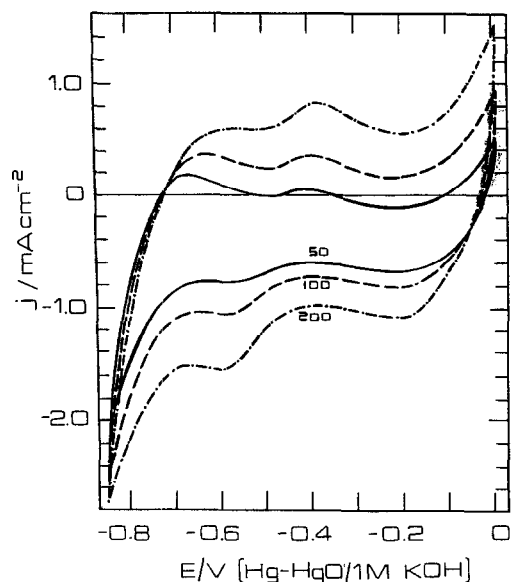


Fig. 7. Cyclic voltammograms on a $\text{Pd}_{96.4}\text{P}_{3.6}$ cathode in 1 M KOH solution, 0.5 atm oxygen partial pressure, 30°C with a rotation rate of 200 rpm. Sweep rates v in V s^{-1} marked on the curves.

the high limiting current density values compared with those obtained with the quasi-steady state techniques are not representative of the actual convective diffusion process.

The voltammogram resulting for the $\text{Au}_{94.0}\text{P}_{6.0}$ electrode in the same electrolyte at 0.75 atm oxygen pressure, 30°C and with rotation rates of 1500, 3000 and 4000 rpm at $5 \times 10^{-3} \text{ V s}^{-1}$ is shown in Fig. 8. The fairly well-defined limiting current densities, taken at -0.55 V after the polarographic maximum for the rest potential, are coincident with those obtained at low sweeping rate. The hysteresis evident in the cathodic runs is apparently

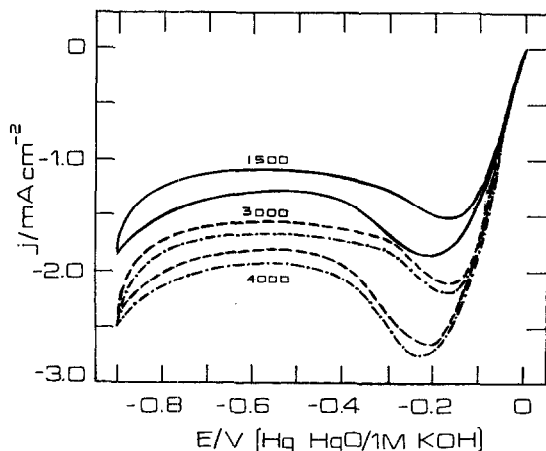


Fig. 8. Cyclic voltammograms on a $\text{Au}_{94.0}\text{P}_{6.0}$ cathode in 1 M KOH solution, 0.75 atm oxygen partial pressure, 30°C. Sweep rate $5 \times 10^{-3} \text{ V s}^{-1}$. Rotation rates in rpm marked on the curves.

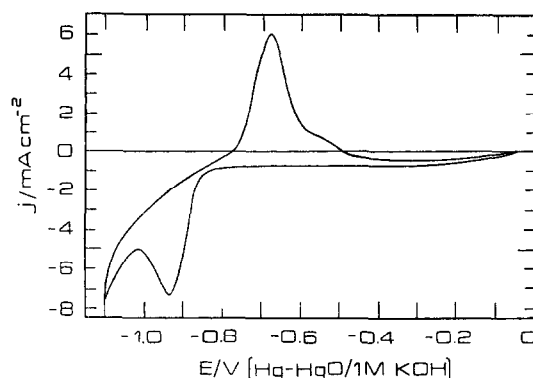


Fig. 9. Cyclic voltammograms on a $\text{Co}_{94.6}\text{P}_{5.4}$ cathode in 1 M KOH solution, 1 atm oxygen partial pressure, 70°C. Sweep rate $5 \times 10^{-3} \text{ V s}^{-1}$ at 1500 rpm.

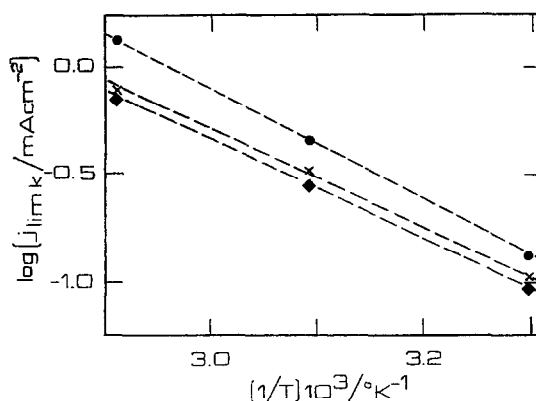


Fig. 10. Temperature dependence of the j_{lim} obtained at the oxygen partial pressure values: ♦, 0.5 atm; x, 0.75 atm and ●, 1.0 atm on $\text{Co}_{94.6}\text{P}_{5.4}$ cathodes. Sweep rate $5 \times 10^{-3} \text{ V s}^{-1}$ at 1500 rpm.

caused by a slow change in the state of the electrode surface. Figure 9 shows the voltammogram obtained with the $\text{Co}_{94.6}\text{P}_{5.4}$ alloy as the cathode in the same electrolyte at 1.0 atm oxygen pressure, 70°C and with a rotation frequency of 1500 rpm and a sweep rate of $5 \times 10^{-3} \text{ V s}^{-1}$. Very well-defined limiting currents independent of the rotation rate were obtained with the potentiodynamic technique at a constant oxygen partial pressure, as shown in Fig. 3.

A possible interpretation for these constant limiting currents is to consider them as limiting kinetic currents resulting from the blockage of the active surface sites by adsorbed species. It is interesting to remark that a linear dependence of these limiting kinetic current densities with the oxygen partial pressures at constant temperature were found. The slopes of the Arrhenius plot in Fig. 10 therefore yields an apparent activation energy of about $43 \pm 5 \text{ kJ mol}^{-1}$; a figure which is in agreement for an activation process.

4. CONCLUSIONS

The following conclusions were drawn from this study:

- The O_2 - η in 1 M KOH solution on $Pd_{96.4}P_{3.6}$ and $Au_{94.0}P_{6.0}$ cathodes is lower with Tafel slopes of -0.065 V dec $^{-1}$ and -0.060 V dec $^{-1}$, respectively.
- The apparent exchange current densities, obtained by extrapolation of the linear regions of the Tafel plots for $Pd_{96.4}P_{3.6}$ and $Au_{94.0}P_{6.0}$ cathodes, vary from 1.5×10^{-5} A cm $^{-2}$ and 5.0×10^{-5} A cm $^{-2}$, respectively.
- Well-defined limiting currents were observed in $Pd_{96.4}P_{3.6}$ and $Au_{94.0}P_{6.0}$ electrodes.
- A limiting kinetic current was found in the $Co_{94.6}P_{5.4}$ amorphous alloy.
- The effect, on the three AMAs, of the presence of oxidized species generated by cyclic voltammetry runs interferes with the mechanisms of OR because the cathodic currents contribute to the reduction of the oxides as well as the reduction of O_2 to HO_2^- ions which react with the oxides causing irreproducible measurements.
- The reaction order with respect to oxygen is unity or AMA I and II.
- The advantage of producing these AMAs by electroless technique as thin coatings on any kind of low cost substrates such as steel should be considered as promising.

Acknowledgements—This research project was financially supported by the Consejo Nacional de Investigaciones Científicas y Técnicas (CONICET) and the Comisión de Investigaciones Científicas de la Provincia de Buenos Aires (CIC). R. C. V. Piatti is a member of the CIC.

REFERENCES

1. Tarasevich, M. R., Sadkowski, A. and Yeager, E., In *Comprehensive Treatise in Electrochemistry*, Vol. 7, eds B. E. Conway, J. O'M. Bockris, E. Yeager, S. U. M. Khan and R. E. White. Plenum Press, New York, 1983.
2. Damjanovic, A., Genshaw, M. A. and Bockris, J. O'M., *Journal of Chemistry and Physics*, 1966, **45**, 4057.
3. Yeager, E., *Electrochimica Acta*, 1986, **29**, 1527.
4. Delahay, P., *Journal of Electrochemical Society*, 1950, **97**, 205.
5. Kreysa, G. and Hakansson, B., *Journal of Electroanalytical Chemistry*, 1986, **201**, 61.
6. Archer, M. D., Corke, C. C. and Harji, B. H., *Electrochimica Acta*, 1987, **32**, 13.
7. Alemu, H. and Jüttner, K., *Electrochimica Acta*, 1988, **33**, 1101.
8. Brossard, L., Schultz, R. and Hout, J. Y., *International Journal of Hydrogen Energy*, 1988, **13**, 251.
9. Budniok, A. and Kupka, J., *Electrochimica Acta*, 1989, **34**, 871.
10. Kupka, J. and Budniok, A., *Journal of Applied Electrochemistry*, 1990, **20**, 1015.
11. Lian, K., Kirk, D. W. and Thorpe, S. J., *Electrochimica Acta*, 1991, **36**, 537.
12. Lian, K., Thorpe, S. J. and Kirk, D. W., *Electrochimica Acta*, 1992, **37**, 2029.
13. Podestá, J. J., Piatti, R. C. V., Arvia, A. J., Edkunge, P., Jüttner, K. and Kreysa, G., *International Journal of Hydrogen Energy*, 1992, **17**, 9.
14. Gorbunova, K. M., Nikiforova, A. A. and Sadakov, G. A., In *Electrochemistry 1966*, ed. M. M. Melnikova. Israel Program for Scientific Translations, Jerusalem, 1970.
15. Pearlstein, F., In *Modern Electroplating*, ed. F. A. Lowenheim. Wiley, New York, 1974.
16. Hoare, J. P., In *Encyclopedia of Electrochemistry of the Elements*, Vol. II, ed. A. J. Bard. Marcel Dekker, New York, 1974.
17. Levich, V. G., *Physicochemical Hydrodynamics*, Prentice Hall, Englewood Cliffs, NJ, 1962.
18. Davis, R. E., Horvath, G. L. and Tobias, C. D., *Electrochimica Acta*, 1967, **12**, 287.
19. Striabel, K. A., McLarnon F. R. and Cairns, E. J., *Journal of the Electrochemical Society*, 1990, **137**, 3351.
20. Gubbins K. and Walker, R., *Journal of the Electrochemical Society*, 1965, **112**, 469.
21. Burke, L. D. and Casey, J. K., *Journal of the Electrochemical Society*, 1993, **140**, 1292.
22. Bolzán, A. E., *Journal of the Electroanalytical Chemistry*, 1995, **380**, 127.
23. Burke, L. D., Cunnane, V. J. and Lee, B. H., *Journal of the Electrochemical Society*, 1992, **139**, 399.
24. Podestá, J. J., Piatti, R. C. V. and Arvia, A. J., *International Journal of Hydrogen Energy*, 1995, **20**, 111.
25. Jayaraman, T. R., Venkatesan, V. K. and Udupa, H. V. K., *Electrochimica Acta*, 1975, **20**, 209.